Supporting Information

A Novel Promising Infrared Nonlinear Optical Selenide $KAg_3Ga_8Se_{14}$ Designed from Benchmark $AgGaQ_2$ (Q = S, Se)

Jia-Nuo Li,[a] Wen-Dong Yao,[a] Xiao-Hui Li,[a] Wenlong Liu,[a] Huai-Guo Xue[a] and Sheng-Ping Guo*[a]

†School of Chemistry & Chemical Engineering, Yangzhou University, Yangzhou, Jiangsu 225002, P. R. China

Experimental Section

Synthesis. The single crystals of $KAg_3Ga_8Se_{14}$ were synthesized by using a high temperature solid-state reaction. The 500 mg mixture of starting materials contain Ag_2O (99.7 %), Ga (99.9 %), Se (99.9 %), B (99 %), and they were stoichiometrically weighed with additional 1 g KI as the reactive flux. The mixture of the starting materials was ground into uniform powder, and then pressed into a pellet, followed by being loaded into quartz tubes. The tube was evacuated to be 1×10^{-4} torr and flame-sealed. Then the tube was put into a muffle furnace, heated from room temperature to 950 ℃ in one day with several intermediate homogenization processes, and kept at 950 ℃ for 7 days, and subsequently cooled to 300 ℃ with a rate of 3 ℃/h, and powered off. The product was washed using distilled water and alcohol more than 3 times followed by being ultrasonic washed. Orange block single crystals of $KAg_3Ga_8Se_{14}$ were obtained and the yield is higher than 90 % based on the mass of Ag. The crystals are stable in the air for several months. As the other products have different colors and shapes, the crystals of $KAg_3Ga_8Se_{14}$ could be easily isolated under an optical microscope.

Structure Determination. The crystallographic data set of $KAg_3Ga_8Se_{14}$ was collected on a Bruker D8 QUEST X-ray diffractometer with graphite-monochromated Mo-Kα radiation (λ

= 0.71073 Å). The structure was solved by Direct Methods and refined by full-matrix least-squares techniques on F^2 with anisotropic displacement parameters for all atoms. All the processes were operated via the Olex2 crystallographic software. The final refinements included anisotropic displacements parameters for all atoms and a secondary extinction correction.[1] The crystallographic parameter data are listed in Table S1. The atomic coordinates, equivalent isotropic displacement parameters, and bond lengths are summarized in Table S2 and Table S3, respectively. The CIF document has also been deposited with the CCDC number of 2038352.

Power X-ray Diffraction (PXRD) Characterization. The purity of $KAg_3Ga_8Se_{14}$ was confirmed by PXRD technique. The PXRD pattern was collected with a Bruker D8 Advance diffractometer at 40 kV and 100 mA for Cu-Kα radiation (λ = 1.5406 Å) with a scan speed of 5 °/min at room temperature. The simulated pattern was obtained using Mercury v3.8 program provided by the Cambridge Crystallographic Data Center and its single-crystal reflection data. The PXRD pattern of $KAg_3Ga_8Se_{14}$ (Fig. S1) corresponds well with the simulated one, indicating a pure sample for $KAg_3Ga_8Se_{14}$.

Infrared (IR) and UV-Vis-NIR Diffuse Reflectance Spectra. The IR spectrum was tested by using a TENSOR27 FT-IR spectrophotometer in the range of 4000–400 cm^{-1}, in which KBr was used as the reference. The diffuse reflectance spectrum was recorded at room temperature on a computer-controlled Cary 5000 UV–Vis–NIR spectrometer equipped with an integrating sphere in the wavelength range of 300–2500 nm. A $BaSO_4$ plate was used as a reference, on which the finely ground powdery sample was coated. The absorption spectrum was calculated from the reflection spectrum by the Kubelka-Munk function.[2]

Thermal Analysis. Differential scanning calorimetry (DSC) analysis on $KAg_3Ga_8Se_{14}$ was performed by using a Mettler Toledo thermal analyzer under a N_2 atmosphere. A 6.77 mg powder sample of $KAg_3Ga_8Se_{14}$ was put into a crucible and heated to 1000 °C and cooled back to room temperature at a rate of 10 °C/min. The product after the thermal analysis was also characterized by PXRD measurement, and the conditions were the same as the above mentioned.

Second-Harmonic Generation (SHG) and Powder Laser Damage Threshold (LDT) Measurements. SHG measurement on powdery crystalline sample of $KAg_3Ga_8Se_{14}$ was

tested by a modified Kurtz-Perry NLO system with a 2.1 μm Q-switch laser radiation as the light source.[3] Polycrystalline powdery sample of $KAg_3Ga_8Se_{14}$ was ground and sieved into particle size ranges of 25~45, 45~75, 75~110, 110~150, 150~210, and 210~250 μm for the size-dependent SHG measurement. Benchmark $AgGaS_2$ (AGS) samples with the same particle size ranges were served as the standards. Each sample was loaded into a customized box that could transmit light and a pulsed IR beam from a Q-switched 2.1 μm laser. The SHG signals were collected by a photomultiplier tube and showed the peaks on the oscilloscope.

The single-pulse measurement method was used to evaluate the LDT value of $KAg_3Ga_8Se_{14}$. The crystalline samples of $KAg_3Ga_8Se_{14}$ and AGS with the same size range 75~110 μm were pressed into glass microscope cover slides and radiated by a 1064 nm laser with a pulse width τ_p of 10 ns in a 1 Hz repetition. The measurements were carried out under an optical microscope once single-pulse radiation passed, and the laser power increased until the damaged spot was observed. Then, the laser power was marked, and the area of the damaged spot was measured as the damage threshold parameters of the sample. The laser beam power was monitored by a Nova II sensor display with a PE50-DIT-C energy sensor. The damaged spot was measured using a Vernier caliper.

Calculation Details. The calculation model was built from the single-crystal diffraction data of $KAg_3Ga_8Se_{14}$. The calculations including band structure, density of states (DOS), and optical properties were carried out using CASTEP module in Material Studio software.[4] The exchange-correlation function GGA (generalized gradient approximation) was chosen and a plane wave basis with the PAW (projector-augmented wave) potentials was used. The plane-wave cutoff energy was 330 eV, and the threshold of 10^{-5} eV was set for the self-consistent-field convergence of the total electronic energy. The electronic configurations for K、Ag、Ga and Se were $4s^1$, $4d^{10}5s^1$, $4s^24p^1$, and $4s^24p^4$, respectively. The numerical integration of the Brillouin zones was performed using 2 × 2 × 3 Monkhorst–Pack *k*-point meshes and the Fermi level at 0 eV was chosen as the reference.

The optical properties described in terms of the complex dielectric function $\varepsilon(\omega) = \varepsilon_1(\omega) + i\varepsilon_2(\omega)$ were calculated. $\varepsilon_1(\omega)$ and $i\varepsilon_2(\omega)$ represent the real and imaginary parts of the dielectric function, respectively.[5,6] $\varepsilon_2(\omega)$ can be used to generate other optical constants using the Kramers-Kroning transform.[7,8] The first-order nonresonant susceptibility at the

low-frequency region is given by $x^{(1)}(\omega) = \varepsilon_1(\omega) - 1$, and the second-order susceptibilities can be expressed in terms of the first-order susceptibilities.[9,10] Refractive index *n* was obtained using the below equation,

$$n(\omega) = \sqrt{\frac{\varepsilon_1^2(\omega)+\varepsilon_2^2(\omega)+\varepsilon_1(\omega)}{2}} \qquad (1)$$

Table S1. Crystal data and structure refinement parameters for $KAg_3Ga_8Se_{14}$.

chemical formula	**$KAg_3Ga_8Se_{14}$**
crystal size (mm^3)	2×1×1
Fw	2025.91
T (K)	296(2)
crystal system	monoclinic
space group	*Cm*
Z	2
unit cell parameters (Å)	a = 12.8805(5) b = 11.6857(4) c = 9.6600(4)
V(Å^3)	1306.87(9)
D_{calcd} (g cm^{-3})	5.148
μ (mm^{-1})	29.945
F(000)	1768
2θ range (º)	4.692 to 54.982
indep. reflns/R_{int}	3130/0.0503
GOF on F^2	0.917
$R1^a$ ($I > 2\sigma(I)$)	0.0250
$wR2^b$ (all data)	0.0525

$^aR1 = ||F_o| - |F_c||/|F_o|$; $^bwR2 = [w(F_o^2 - F_c^2)^2]/[w(F_o^2)^2]^{1/2}$.

Table S2. Atomic coordinates ($\times 10^4$) and equivalent isotropic displacement parameters (U_{eq}[a], $Å^2 \times 10^3$) for $KAg_3Ga_8Se_{14}$.

Atom	*x*	*y*	*z*	U_{eq}/Å^2
K(1)	-7338(4)	-5000	-2976(5)	52.6(16)
Ag(1)	-3104.4(10)	-5000	-3698.1(13)	27.6(3)
Ag(2)	-6030.3(10)	-10000	-5756.9(12)	27.9(3)
Ag(3)	-3868.1(10)	-10000	-8206.2(13)	26.2(3)
Ga(1)	-1994.8(8)	-6659.4(8)	18.2(10)	10.8(2)
Ga(2)	-6092.9(9)	-6698.5(7)	-5950.2(12)	11.2(2)
Ga(3)	-4028.8(8)	-6711.5(8)	-7996.0(10)	11.0(2)
Ga(4)	-5058.2(9)	-8351.1(8)	-2048.3(12)	11.6(2)
Se(1)	-2001.9(7)	-6930.7(7)	-2429.1(10)	12.51(18)
Se(2)	-3054.0(8)	-8247.1(8)	-6347.1(10)	12.7(2)
Se(3)	-5352.8(10)	-5000	-4441.2(14)	11.7(3)
Se(4)	-4044.2(7)	-6628.8(7)	-10518.9(9)	10.30(19)
Se(5)	-3892.3(10)	-10000	-885.8(14)	12.6(3)
Se(6)	-4867.7(8)	-8188.6(8)	-4397.7(10)	11.65(19)
Se(7)	-6066.9(8)	-6631.2(7)	-8495.2(10)	10.05(18)
Se(8)	-3244.9(11)	-5000	-6579.2(14)	13.3(3)
Se(9)	-6059.3(11)	-10000	-8557.8(13)	13.6(3)

[a] U_{eq} is defined as one third of the trace of the orthogonalized U_{ij} tensor.

Table S3. Important bond lengths (Å) for $KAg_3Ga_8Se_{14}$.

Bond	Distance/Å	Bond	Distance/Å
K(1)–Se(1)	3.6235(10)	Ag(3)–Se(5)#6	2.5749(14)
K(1)–Se(1)#2	3.6235(10)	Ag(3)–Se(9)	2.6905(16)
K(1)–Se(2)	3.609(4)	Ga(1)–Se(1)	2.3815(12)
K(1)–Se(2)#2	3.609(4)	Ga(1)–Se(4)#7	2.4572(12)
K(1)–Se(3)	3.423(4)	Ga(1)–Se(7)#8	2.4446(13)
K(1)–Se(5)#2	3.409(4)	Ga(1)–Se(9)#9	2.3773(11)
K(1)–Se(6)#2	3.614(4)	Ga(2)–Se(2)#1	2.3840(14)
K(1)–Se(6)	3.614(4)	Ga(2)–Se(3)	2.3990(12)
Ag(1)–Se(1)	2.6615(10)	Ga(2)–Se(6)	2.3868(13)
Ag(1)–Se(1)#3	2.6615(10)	Ga(2)–Se(7)	2.4744(13)
Ag(1)–Se(3)	2.6609(15)	Ga(3)–Se(2)	2.3622(13)
Ag(1)–Se(8)	2.7085(16)	Ga(3)–Se(4)	2.4306(13)
Ag(2)–Se(6)#4	2.5928(11)	Ga(3)–Se(7)	2.4541(11)
Ag(2)–Se(6)	2.5928(11)	Ga(3)–Se(8)	2.3836(12)
Ag(2)–Se(8)#5	2.6043(17)	Ga(4)–Se(1)#1	2.3883(13)
Ag(2)–Se(9)	2.6897(17)	Ga(4)–Se(4)#7	2.4993(12)
Ag(3)–Se(2)	2.6209(12)	Ga(4)–Se(5)	2.3982(12)
Ag(3)–Se(2)#4	2.6209(12)	Ga(4)–Se(6)	2.3951(12)

Symmetry codes: #1 -1/2+*x*, -3/2-*y*, +*z*; #2 -1/2+*x*, 1/2+*y*, +*z*; #3 +*x*, -1-*y*, +*z*; #4 +*x*, -2-*y*, +*z*; #5 -1/2+*x*, -1/2+*y*, +*z*; #6 +*x*, +*y*, -1+*z*; #7 +*x*, +*y*, 1+*z*; #8 1/2+*x*, -3/2-*y*, 1+*z*; #9 1/2+*x*, 1/2+*y*, 1+*z*.

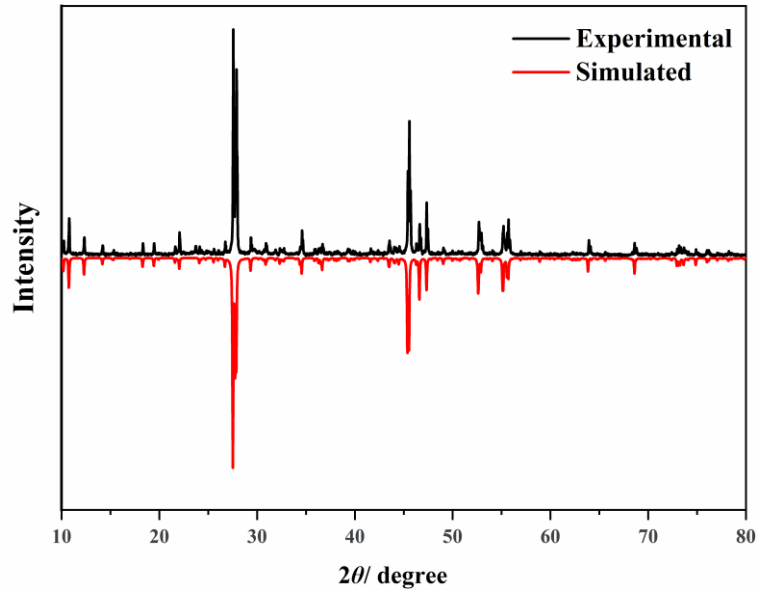

Fig. S1 Powder X-ray diffraction pattern for $KAg_3Ga_8Se_{14}$.

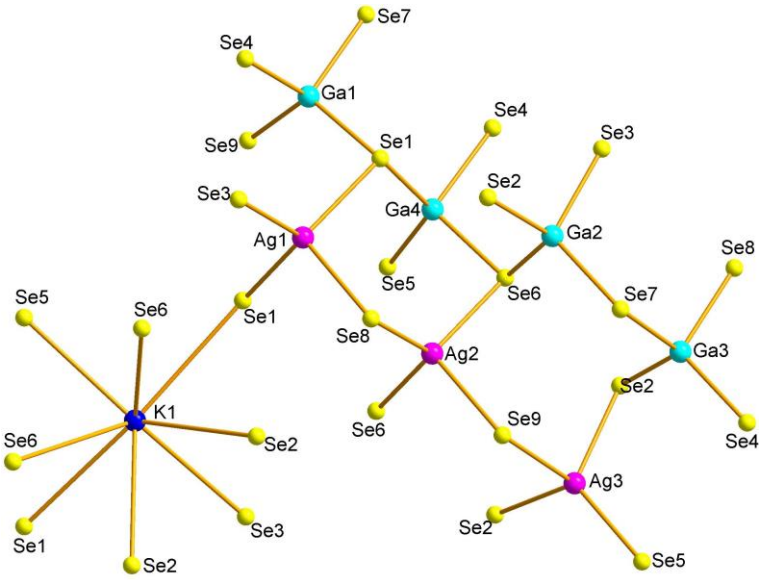

Fig. S2 Coordination geometry of $KAg_3Ga_8Se_{14}$.

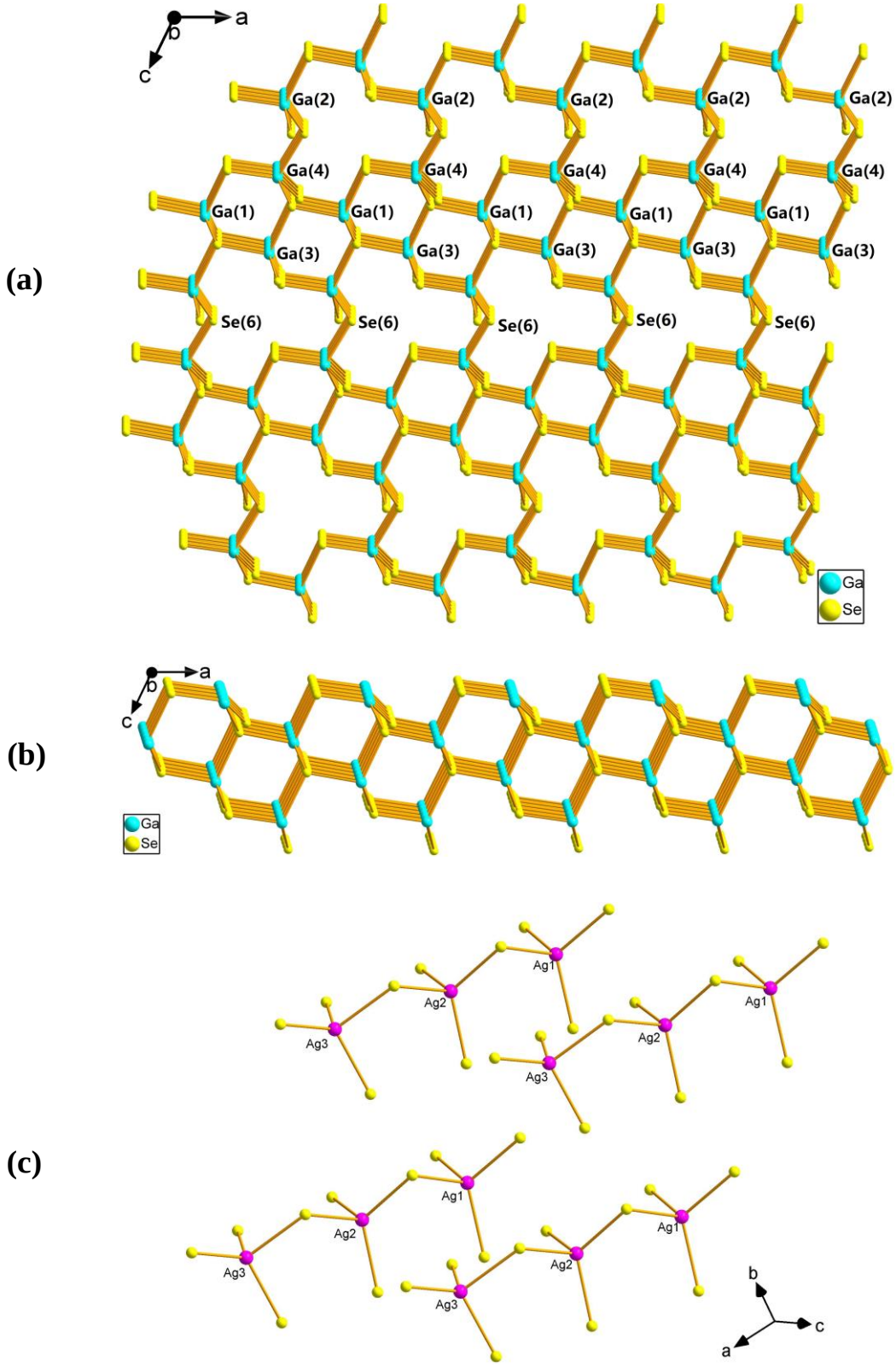

Fig. S3 (a) $GaSe_4$ tetrahedra constructed the 3*D* framework; (b) Honeycomb-like layers along the *a*-axis if Se(6) atoms omitted; (c) $AgSe_4$ tetrahedra constructed $[Ag_3Se_{10}]^{17-}$ trimers.

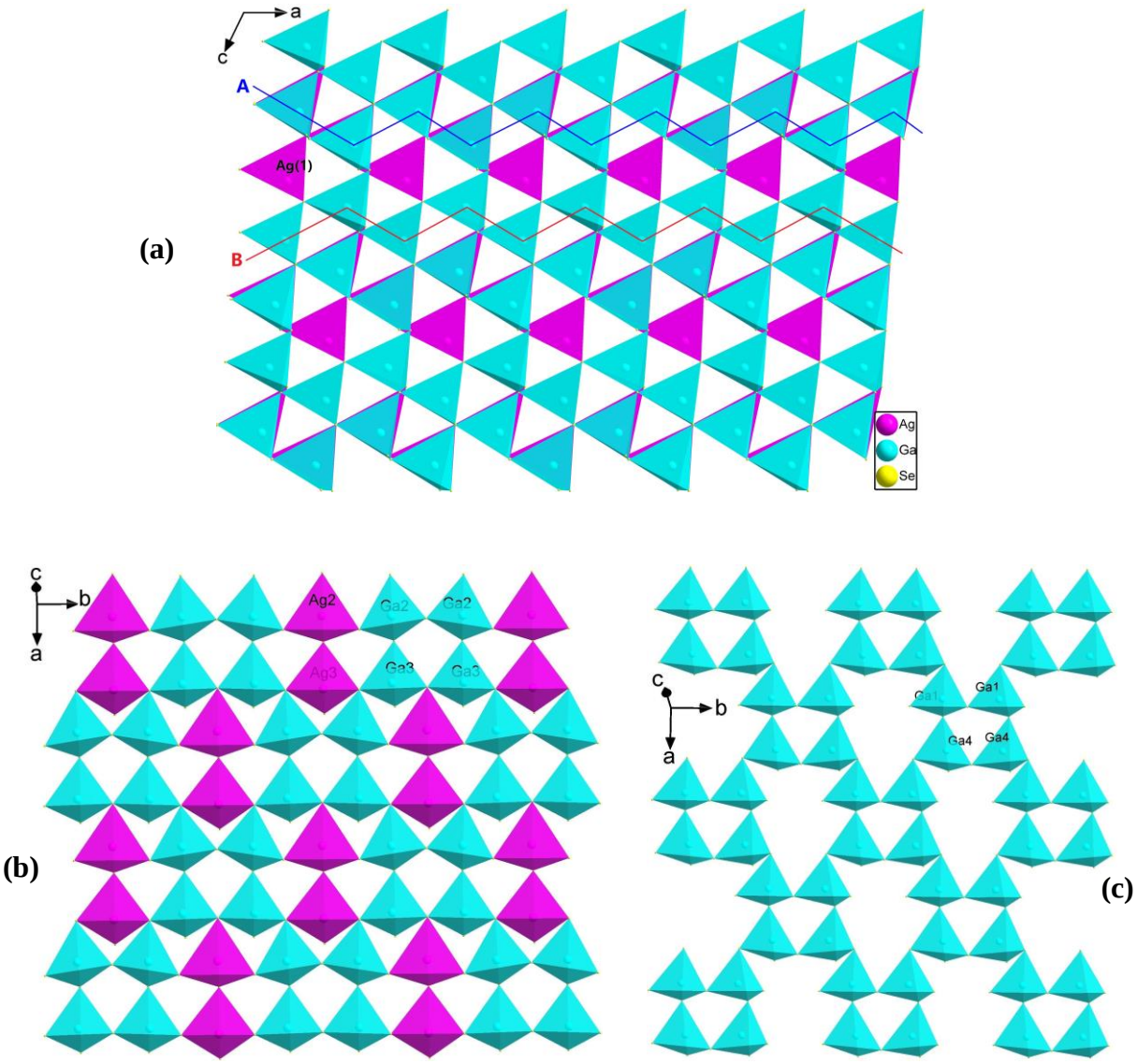

Fig. S4 (a) Ag−Ga−Se built 3*D* structural motif, which is comprised of corrugated layers A and B and $Ag(1)Se_4$ tetrahedra; (b) Corrugated layer A viewed along the *c*-axis; (c) Corrugated layer B viewed along the *c*-axis.

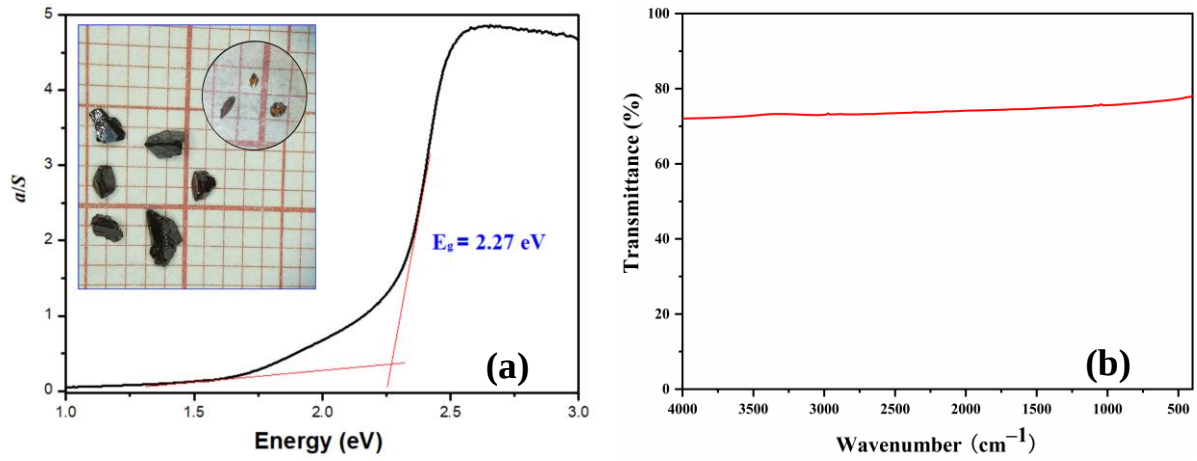

Fig. S5 (a) UV-Vis-NIR diffuse reflectance spectrum of $KAg_3Ga_8Se_{14}$ and its crystal photos. (b) Fourier transform infrared spectrum of $KAg_3Ga_8Se_{14}$ measured from 400 to 4000 cm^{-1}.

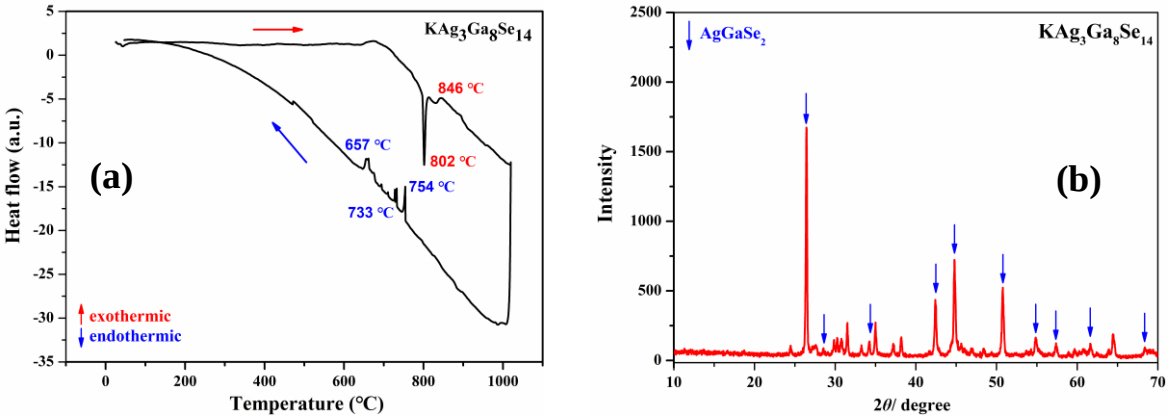

Fig. S6 (a) DSC curve for $KAg_3Ga_8Se_{14}$ measured from room temperature to 1000 °C. (b) PXRD pattern of $KAg_3Ga_8Se_{14}$ after DSC measurement.

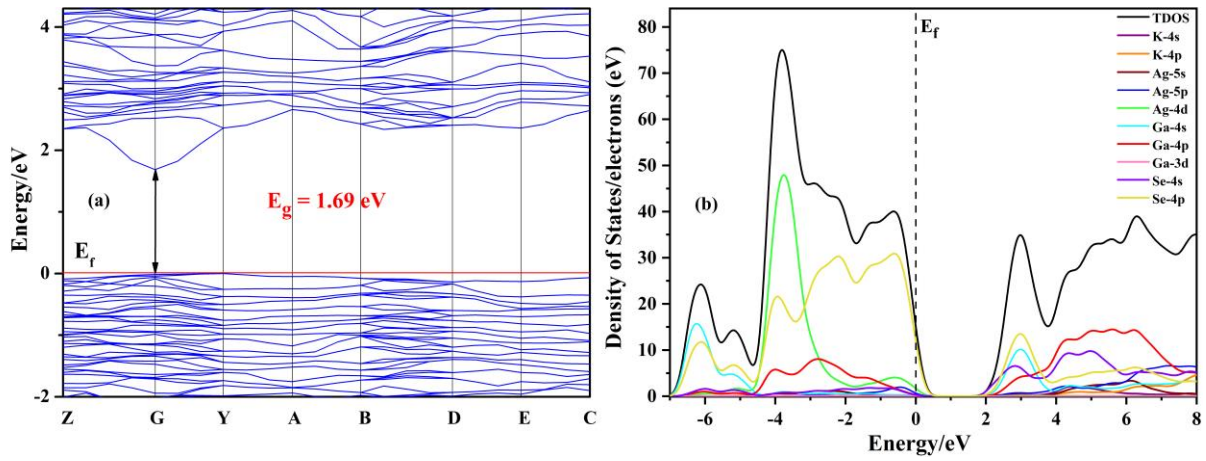

Fig. S7 Calculated band structure (a) and density of states (DOS, b) for $KAg_3Ga_8Se_{14}$. Fermi level is chosen at 0 eV.

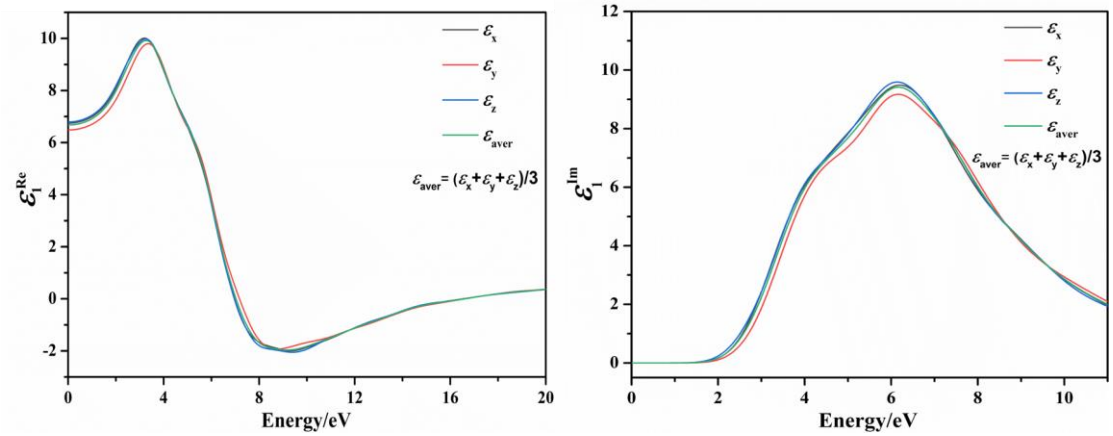

Fig. S8 Calculated real and imaginary parts of optical dielectric constants for $KAg_3Ga_8Se_{14}$.

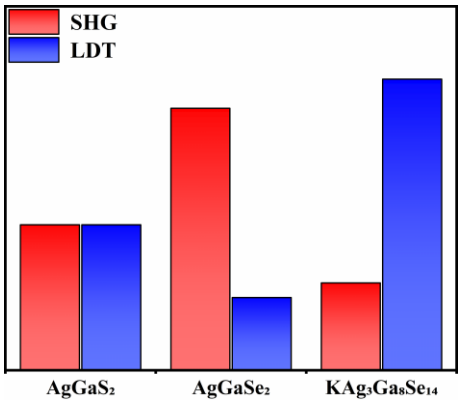

Fig. S9 SHG effects and LDT comparison between $KAg_3Ga_8Se_{14}$, $AgGaS_2$, and $AgGaSe_2$.

1 G. M. Sheldrick, *Acta Crystallogr. C*, 2015. **71**, 3−8.

2 (a) W. W. Wendlandt and H. G. Hecht, *Reflectance Spectroscopy*, Interscience Publishers, New York, **1966**; (b) G. Kortüm, *Reflectance Spectroscopy*, Springer, 1969.

3 S. K. Kurtz and T. T. Perry, *J. Appl. Phys.*, 1968, **39**, 3798−3813.

4 S. J. Clark, M. D. Segall, C. J. Pickard, P. J. Hasnip, M. I. Probert, K. Refson and M. C. Payne, *Z. Kristallogr.-Cryst. Mater.*, 2005, **220**, 567−570.

5 F. Bassani and G. P. Parravicini, *Electronic States and Optical Transitions in Solid*s; Pergamon Press Ltd.: Oxford, U.K., 1976.

6 M. Gajdoš, K. Hummer, G. Kresse, J. Furthmüller and F. Bechstedt, *Phys. Rev. B*, 2006, **73**, 045112.

7 S. Laksari, A. Chahed, N. Abbouni, O. Benhelal and B. Abbar, *Comp. Mater. Sci.*, 2006, **38**, 223−230.

8 S. D. Mo and W. Y. Ching, *Phys. Rev. B*, 1995, **51**, 13023.

9 C. S. Aversa and J. E. Sipe, *Phys. Rev. B*, 1995, **52**, 14636.

10 S. N. L. Rashkeev, W. R. L. Lambrecht and B. Segall, *Phys. Rev. B*, 1998, **57**, 3905.